Wiener estimation of the Green's function

GEOPHYSICS, VOL. 78, NO. 5 (SEPTEMBER-OCTOBER 2013); P. W31–W44, 18 FIGS.
10.1190/GEO2013-0032.1

Wiener estimation of the Green's function

Anton Ziolkowski[1]

ABSTRACT

I consider the problem of finding the impulse response, or Green's function, from a measured response including noise, given an estimate of the source time function. This process is usually known as signature deconvolution. Classical signature deconvolution provides no measure of the quality of the result and does not separate signal from noise. Recovery of the earth impulse response is here formulated as the calculation of a Wiener filter in which the estimated source signature is the input and the measured response is the desired output. Convolution of this filter with the estimated source signature is the part of the measured response that is correlated with the estimated signature. Subtraction of the correlated part from the measured response yields the estimated noise, or the uncorrelated part. The fraction of energy not contained in this uncorrelated component is defined as the quality of the filter. If the estimated source signature contains errors, the estimated earth impulse response is incomplete, and the estimated noise contains signal, recognizable as trace-to-trace correlation. The method can be applied to many types of geophysical data, including earthquake seismic data, exploration seismic data, and controlled source electromagnetic data; it is illustrated here with examples of marine seismic and marine transient electromagnetic data.

INTRODUCTION

In data from seismic, acoustic, and electromagnetic sources, the measured response is a convolution of the source time function with the Green's function, or impulse response, plus noise. In analysis of these data, it is often desired to obtain an accurate measure of the Green's function, or impulse response, given an estimate of the source time function. In exploration geophysics, this is known as *signature deconvolution*.

Classical signature deconvolution (Rice, 1962; Robinson, 1967; Robinson and Treitel, 1967; Jovanovich et al., 1983) designs an inverse filter for the estimated source signature and convolves the filter with the measured data to obtain an estimate of the earth impulse response. The filter is recalculated when the estimated source signature changes. This basic concept has been used for decades in exploration seismology. The quality of the deconvolved result is uncertain.

The use of Wiener's theory to tackle the problem has long been associated with the predictive deconvolution approach of Peacock and Treitel (1969), based on Robinson's (1954) model of the seismogram, in which the measured response is the convolution of a basic wavelet with an uncorrelated series identified with the reflection coefficients of the layered earth. In one realization, the basic wavelet might be a reverberating pulse train. At the heart of this approach are the assumptions that the reflection response of the earth is white and the basic wavelet is minimum phase, although it was never claimed that these assumptions are necessarily correct. They were made to make the problem tractable: the autocorrelation of the wavelet is then the same as the autocorrelation of the seismogram, apart from a scale factor, and the minimum-phase assumption then uniquely determines the wavelet from its autocorrelation.

In the early days of onshore seismic exploration with dynamite, the minimum-phase assumption was probably correct. With the developments of the vibroseis method and marine seismic exploration, the minimum-phase assumption has been found to be too restrictive. It has also been shown that the reflection response of the earth is not white (Fokkema and Ziolkowski, 1987) and, therefore, the autocorrelation of the seismogram is not the same as the autocorrelation of the basic wavelet apart from a scale factor.

This paper uses Wiener's (1949) theory to formulate recovery of the earth impulse response as the calculation of the optimum filter which, convolved with the estimated source signature, yields the best least-squares estimate of the measured response. There is thus a separate Wiener filter calculation for each data trace. Convolution of this filter with the estimated source signature is the component of the measured response that is correlated with the estimated signature. Subtraction of the correlated component from the measured

Manuscript received by the Editor 27 January 2013; revised manuscript received 17 April 2013; published online 5 August 2013.
[1]University of Edinburgh, School of Geosciences, Grant Institute, Edinburgh, UK. E-mail: Anton.Ziolkowski@ed.ac.uk.

data yields the uncorrelated component: the estimated noise. The Wiener filter minimizes the energy of the estimated noise, by definition. The quality of the filter is defined as "the fraction of energy in the measured signal not contained in the estimated noise". If the estimated source signature contains errors, the estimated earth impulse response is incomplete, and the estimated noise contains signal, which can be recognized as trace-to-trace correlations.

The convolutional model for the measured data and the classical inverse-filter approach to signature deconvolution are reviewed first. The design of the Wiener filter is reviewed next. This is followed by a brief review of the application of Wiener filters to predictive deconvolution, inverse filtering, and signature deconvolution. Then, the application of the Wiener optimization approach to the estimation of the Green's function is presented; this is the novel part of the paper. Finally, the method is applied to synthetic and real marine seismic and marine transient electromagnetic data to show how it works.

CONVOLUTIONAL MODEL AND CLASSICAL SIGNATURE DECONVOLUTION

Consider a geophysical experiment to investigate the earth using an active source and passive receivers. For example, this could be a seismic experiment or a transient electromagnetic experiment. Seismic wave propagation is a linear process because Hooke's law is obeyed, i.e., stress is proportional to strain. Electromagnetic propagation is a linear process because Maxwell's equations are linear and Ohm's law is obeyed, i.e., voltage is proportional to current. In both cases, the earth can be treated as a linear time-invariant system, because the medium parameters can be considered constant over the duration of the experiment.

In the setup illustrated in Figure 1, and using the well-known notation of Robinson and Treitel (1967), let the digital measurement at a receiver be

$$V_t = s_t * g_t + n_t, \tag{1}$$

where s_t is the source signature, g_t is the earth impulse response, the asterisk denotes convolution, and n_t is the noise and is what would be measured if there were no geophysical experiment; the subscript t denotes the time sample. The impulse response g_t is also known as the Green's function. It depends on the source position (x_s, y_s, z_s) and the receiver position (x_r, y_r, z_r), as well as time t. The positional dependencies are noted, but are not included in the following equations, as they are not needed for the argument.

In this description, the source is assumed to be small compared with a wavelength at all measured frequencies and the source time function is then the same in all directions. In many situations, however, the source time function varies with direction. This occurs, e.g., with electric dipole sources and with sources that are not small compared with a wavelength at high frequencies, including vibrator arrays onshore, air gun arrays offshore, and large earthquake sources. This issue is not addressed directly in this paper, but there is an indication in the air gun example presented later that directivity effects are significant.

Normally the source signature is not known exactly. An estimate $\hat{s}_t$ of the signature is obtained by measurements, by modeling, or by some other means (e.g., Ziolkowski, 1984; Osman and Robinson, 1996), such that there may be an error in every sample,

$$\hat{s}_t = s_t - es_t, \tag{2}$$

where es_t is the unknown error. It is possible that there is also a convolutional error — for example, an instrument filter — but that is ignored here. Classical signature deconvolution (e.g., Robinson and Treitel, 1967) finds an approximate inverse filter f_t of $\hat{s}_t$ such that

$$f_t * \hat{s}_t = d_t, \tag{3}$$

where d_t is a known band-limited impulse. Signature deconvolution is then the result of the convolution of this approximate inverse filter with the measurement

$$\begin{aligned} f_t * V_t &= f_t * s_t * g_t + f_t * n_t \\ &= f_t * (\hat{s}_t + es_t) * g_t + f_t * n_t \\ &= d_t * g_t + f_t * es_t * g_t + f_t * n_t \end{aligned} \tag{4}$$

in which equations 2 and 3 have been used.

The first term on the right-hand side of equation 4 is the required result: It is the true, unknown, earth impulse response convolved with the known bandlimited impulse; the second term is an error caused by uncertainty in the source signature estimate; the third term is the convolution of the approximate inverse filter with the noise. It is well known (e.g., Rice, 1962; Stoffa and Ziolkowski, 1983) that this noise term is dependent on the design of the bandlimited impulse d_t; for example, if $d_t = \delta_t$, a perfect digital impulse, the noise blows up at frequencies where the estimated signature $\hat{s}_t$ has little or no energy.

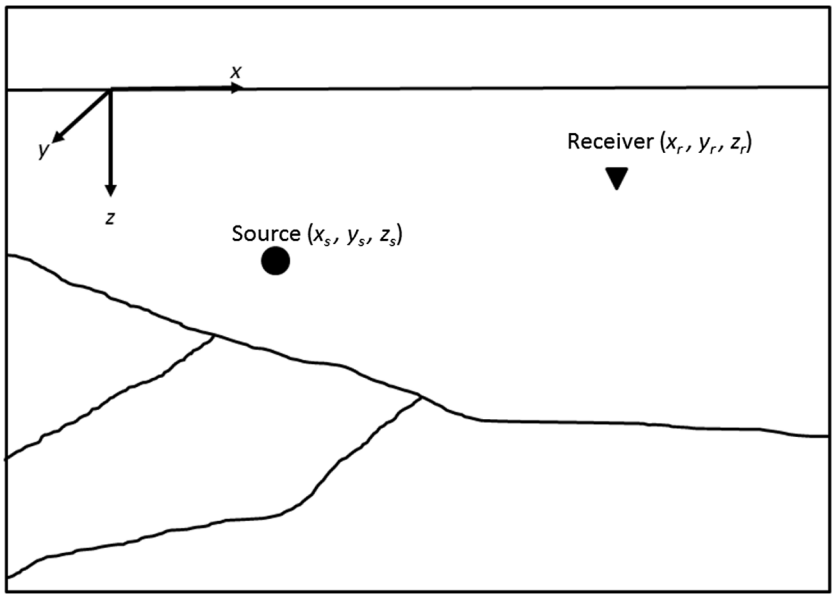

Figure 1. Source and receiver in the earth. The impulse response at the receiver, or Green's function, is a function of the source position (x_s, y_s, z_s), the receiver position (x_r, y_r, z_r), and time t.

It is not known how the second and third terms compare with the desired first term. That is, we are not able to distinguish these terms in the deconvolved data and we are unable to quantify the quality of the deconvolution. Armed with the same information, the approach proposed below also allows the signal and noise to be estimated as well as separated, allowing the quality of the deconvolution to be determined.

THE WIENER FILTER

The Wiener filter has been used extensively in geophysical data processing, following the pioneering work of Robinson (1954) and Robinson and Treitel (1967). The notation of Robinson and Treitel (1967) is adopted, and Figure 2, showing the general filter design model, is redrawn from Figure 1 of their paper. The object is to design a causal linear digital filter

$$f_t = f_0, f_1, f_2 \cdots, f_j, \cdots, f_n,$$

which, convolved with the input signal x_t, yields the best least-squares estimate of the desired output signal z_t. The actual output signal is $y_t = x_t * f_t$. The error at sample t is $(z_t - y_t)$, and the sum of the squares of the errors is

$$I = \sum_t (z_t - y_t)^2 = \sum_t (z_t - x_t * f_t)^2. \tag{5}$$

The quantity I is minimized by setting

$$\frac{\partial I}{\partial f_j} = 0, \qquad j = 0, 1, 2, \cdots, n. \tag{6}$$

This leads to the so-called "normal" equations

$$\sum_{\tau=0}^{n} f_\tau \phi_{xx}(j - \tau) = \phi_{zx}(j), \quad \text{for } j = 0, 1, 2, \ldots, n, \tag{7}$$

where $\phi_{xx}(\tau)$ is the autocorrelation of the input signal x_t, and $\phi_{zx}(\tau)$ is the crosscorrelation of the desired output signal z_t with the input signal x_t

$$\phi_{xx}(\tau) = \sum_t x_t x_{t-\tau} \tag{8}$$

$$\phi_{zx}(\tau) = \sum_t z_t x_{t-\tau}. \tag{9}$$

Levinson (1946) and Robinson and Treitel (1967) show that a convenient expression for the error energy can be found when the normal equations are divided by the zero-lag coefficient of the autocorrelation of the desired output $\phi_{zz}(0) = \sum_t z^2$ and, using the property that the autocorrelation of real signals is symmetric, $\phi_{xx}(\tau) = \phi_{xx}(-\tau)$, equations 7 may be written as

$$\begin{bmatrix} a_0 & a_1 & \cdots & a_n \\ a_1 & a_0 & \cdots & a_{n-1} \\ \vdots & \vdots & \cdots & \vdots \\ a_n & a_{n-1} & \cdots & a_0 \end{bmatrix} \begin{bmatrix} f_0 \\ f_1 \\ \vdots \\ f_n \end{bmatrix} = \begin{bmatrix} b_0 \\ b_1 \\ \vdots \\ b_n \end{bmatrix}, \tag{10}$$

with

$$a_\tau = \frac{\phi_{xx}(\tau)}{\phi_{zz}(0)}, \tag{11}$$

$$b_\tau = \frac{\phi_{zx}(\tau)}{\phi_{zz}(0)}. \tag{12}$$

Levinson (1946) develops a fast solution of these equations.

The error I is minimum, by definition. As shown by Levinson (1946) and Robinson and Treitel (1967), the normalized mean square error can be expressed as

$$\varepsilon = \frac{I_{MIN}}{\phi_{zz}(0)} = 1 - \sum_{\tau=0}^{n} f_\tau b_\tau. \tag{13}$$

As stated by Robinson and Treitel (1967): "Since ε is a sum of squares it can never be negative. Moreover, ε can never be greater than unity, because the value 1 for ε can always be obtained by letting the filter f_τ be identically zero. Hence, we have that

$$0 \le \varepsilon \le 1. \tag{14}$$

As noted by Levinson (1946), the quality of the filter may be defined as the complementary quantity

$$q = 1 - \varepsilon = \sum_{\tau=0}^{n} f_\tau b_\tau, \tag{15}$$

with

$$0 \le q \le 1. \tag{16}$$

The smaller the error, the higher the value of q. If $q = 1$, the error is zero and the filter is perfect.

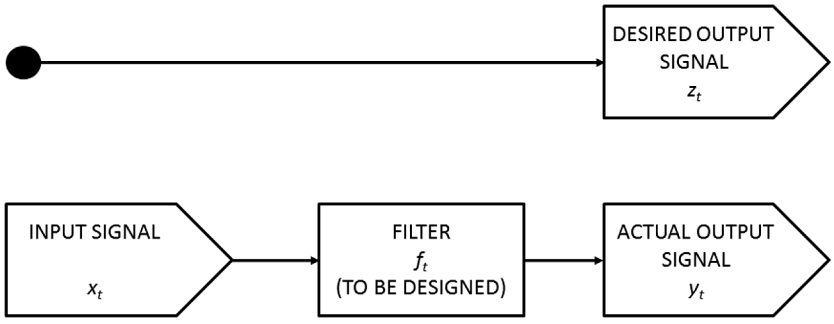

Figure 2. The general filter design model (redrawn from Figure 1, Robinson and Treitel, 1967)

THE WIENER FILTER IN DECONVOLUTION

This section briefly reviews predictive deconvolution, inverse filtering, and signature deconvolution to establish the difference between the proposed application and earlier work. Each application affects only the choice of input and desired output signals in the design of the Wiener filter.

Predictive deconvolution and inverse filtering

In their landmark paper, Peacock and Treitel (1969) propose predictive deconvolution for suppression of reverberations and inverse filtering of seismic data. The underlying model is that the seismogram is the convolution of a basic wavelet with an uncorrelated (white) series that can be identified with the reflection coefficient series of a layered medium, as proposed by Robinson (1954). The autocorrelation of the seismogram is then the same as the autocorrelation of the basic wavelet, apart from a scale factor. First, a *prediction* filter is defined. Convolution of the prediction filter with the seismogram x_t predicts the seismogram $x_{t+\alpha}$ at a later time $t+\alpha$ using time samples up to time t, but not later. In the design of the Wiener filter, the input signal is the seismogram x_t, and the desired output is the time-advanced version of the seismogram $x_{t+\alpha}$. Because the seismogram has already been recorded, these quantities are known and the "prediction" is based on the autocorrelation of the recorded seismogram. Subtraction of the predicted value $\hat{x}_{t+\alpha}$, say, from the measured value $x_{t+\alpha}$ yields the reflection coefficient, apart from a scale factor. Peacock and Treitel show how a *prediction-error* filter could be constructed from the prediction filter to yield the reflection coefficient series directly. The prediction parameter α determines the compression of the wavelet: The smaller the value of α, the sharper the events. Peacock and Treitel show that choosing $\alpha = 1$ reduces the prediction-error filter to the inverse of the basic wavelet, apart from a scale factor, provided the wavelet is minimum phase.

For about twenty years, this approach to deconvolution and multiple suppression was the workhorse of the industry. Gradually, however, the whiteness assumption for the reflection coefficients and the minimum-phase assumption for the wavelet were found to be too restrictive.

Signature deconvolution

Robinson and Treitel (1967) show very clearly how the Wiener filter approach can be used to shape a wavelet, $\hat{s}_t$ say, into a shorter, sharper wavelet, d_t say. In this case, the input signal for the Wiener filter design is $\hat{s}_t$, and the desired output signal is d_t. In the limit, d_t can be the Kroneker delta δ_t. As mentioned above, there is no measure of the quality of the result.

WIENER ESTIMATION OF THE GREEN'S FUNCTION

To use the Wiener filter to estimate the Green's function directly, the estimated source time function is the input signal $x_t = \hat{s}_t$, and the measured response at the receiver is the desired output signal $z_t = V_t$. The resulting normal equations are then

$$\begin{bmatrix} A_0 & A_1 & \cdots & A_n \\ A_1 & A_0 & \cdots & A_{n-1} \\ \vdots & \vdots & \cdots & \vdots \\ A_n & A_{n-1} & \cdots & A_0 \end{bmatrix} \begin{bmatrix} \hat{g}_0 \\ \hat{g}_1 \\ \vdots \\ \hat{g}_n \end{bmatrix} = \begin{bmatrix} B_0 \\ B_1 \\ \vdots \\ B_n \end{bmatrix}, \tag{17}$$

where the Wiener filter $\hat{g}_t$ is the estimate of the Green's function g_t, A_τ is the normalised autocorrelation of $\hat{s}_t$,

$$A_\tau = \frac{\sum_t \hat{s}_t \hat{s}_{t-\tau}}{\sum_t V_t^2}, \tag{18}$$

and B_τ is the normalized crosscorrelation of V_t with $\hat{s}_t$,

$$B_\tau = \frac{\sum_t V_t \hat{s}_{t-\tau}}{\sum_t V_t^2}. \tag{19}$$

Convolution of $\hat{s}_t$ with $\hat{g}_t$ gives the best least-squares match to the data, by definition, and is

$$\begin{aligned} y_t &= \hat{s}_t * \hat{g}_t \\ &= (s_t - es_t) * (g_t - eg_t) \\ &= s_t * g_t - s_t * eg_t - es_t * g_t - es_t * eg_t. \end{aligned} \tag{20}$$

Subtracting equation 20 from equation 1 yields an estimate of the noise, which is

$$V_t - y_t = \hat{n}_t = n_t + s_t * eg_t + es_t * g_t + es_t * eg_t. \tag{21}$$

The terms on the right-hand side of equation 21 are all unknown. The first term is the true noise; the second term is caused by the error in the estimated Green's function, caused, in turn, by the original error in the estimated source signature; the third term is caused by the systematic error in the source signature estimate and looks like signal; the fourth term is a second-order error caused by the source signature error and the error in the Green's function.

Following the definition in equation 15, the quality factor of the estimated Green's function may be defined as

$$q = \sum_{\tau=0}^{n} \hat{g}_\tau B_\tau. \tag{22}$$

This is a number between zero and unity; the closer it is to unity, the better is the result. Clearly, the quality of the result increases with the quality of the estimate of the source time function.

In the solution of equations 17 it is well known that it may be necessary to increase the value of A_0 by a small amount, typically of the order of 1%. This is known as "adding white noise" (e.g., Ziolkowski [1984], Chapter 5). The best value is found by trial and error: It is the smallest value that gives a stable response.

APPLICATION TO SYNTHETIC DATA

Wedge model, PRBS signature, and air gun signature

A simple wedge model and two signatures are used to illustrate the method. The model has been chosen for its simplicity and to illustrate resolution of events down to a single sample. A real deghosted air gun signature has been chosen to show what is possible with today's marine seismic technology. One period of a pseudorandom binary sequence (PRBS) is used to illustrate what is possible with a realizable source with almost ideal spectral characteristics. The use of PRBS is well established in electromagnetic applications; it was first used in exploration applications by Duncan et al. (1980). A PRBS is ideal for electromagnetic applications because the power is constant while the source is on, and switching the polarity of the current can be achieved in the order of a microsecond. It also has great appeal for the seismic vibroseis method, but the inertia of the baseplate and reaction masses pose formidable problems for the rapid reversal of the applied force.

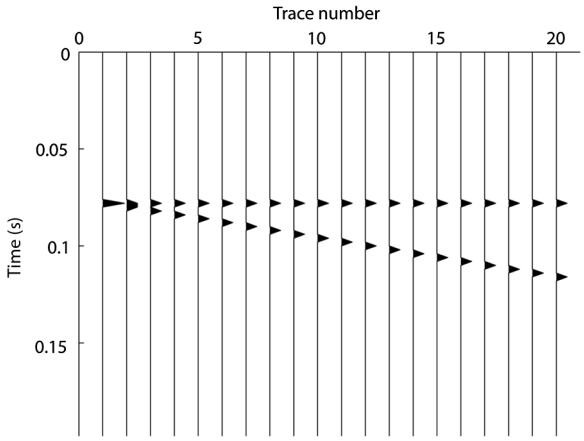

Figure 3. Wedge model with horizontal reflector at 0.078 s, with event below, dipping at one sample per trace.

Figure 3 shows the simple time-domain wedge model, sampled at 0.002 s, consisting of a horizontal event at 0.078 s, shown on 20 traces, and an event dipping from left to right at one sample per trace. The plotting is by conventional variable area display. Each event consists of a single sample of amplitude 1, with zeros before and after; that is, an event at time τ is a Kroneker delta $\delta_{t-\tau}$. On trace 1, the two events are coincident, so the amplitude is 2 at 0.078 s.

Figure 4a shows the first signature, an order 7 PRBS signature p_t. A PRBS is a signal that switches between two levels at pseudorandom times. The signal is generated in a computer using principles that were established in the 1950s (Golomb, 1955, 1982; Zierler, 1959). In this case, the two levels are $+1$ A and -1 A, and the switch times are pseudorandom multiples of the sampling interval $\Delta t = 0.002$ s. A PRBS normally is periodic. Here, a single period is used. The length of one period of a PRBS is $N = 2^n - 1$ samples, with n the order of the sequence; in this case, $n = 7$ and $N = 127$. Figure 4b shows the amplitude spectrum of Figure 4a; that is, Figure 4b shows $|P_k|$, for $k = 0, 1, \cdots, (N-1)/2$, and P_k is the discrete Fourier transform of p_t,

$$P_k = \Delta t \sum_{t=0}^{N-1} p_t \exp\{2\pi i t k/N\}. \tag{23}$$

It can be seen that the amplitude spectrum is flat, except at DC, or 0 Hz, where it has a value 0.002 because the difference between the number of positive and negative values is modulus 1.

Figure 5a shows an estimated far-field signature sa_t from a compact air gun array, which is used later in the filtering of real seismic data. It is employed here to show its properties in contrast to the PRBS. The signature has a very sharp initial peak, followed by subsequent bubble oscillations. The sea surface reflection, or "source ghost" has been removed. This broadens the spectrum and enhances the bubble oscillations, but better represents the signal of a monopole source. Notice the signature has a delay relative to $t = 0$. Figure 5b shows the amplitude spectrum of the signature SA_k plotted on a logarithmic scale versus linear frequency, to show the effect of the antialias filter.

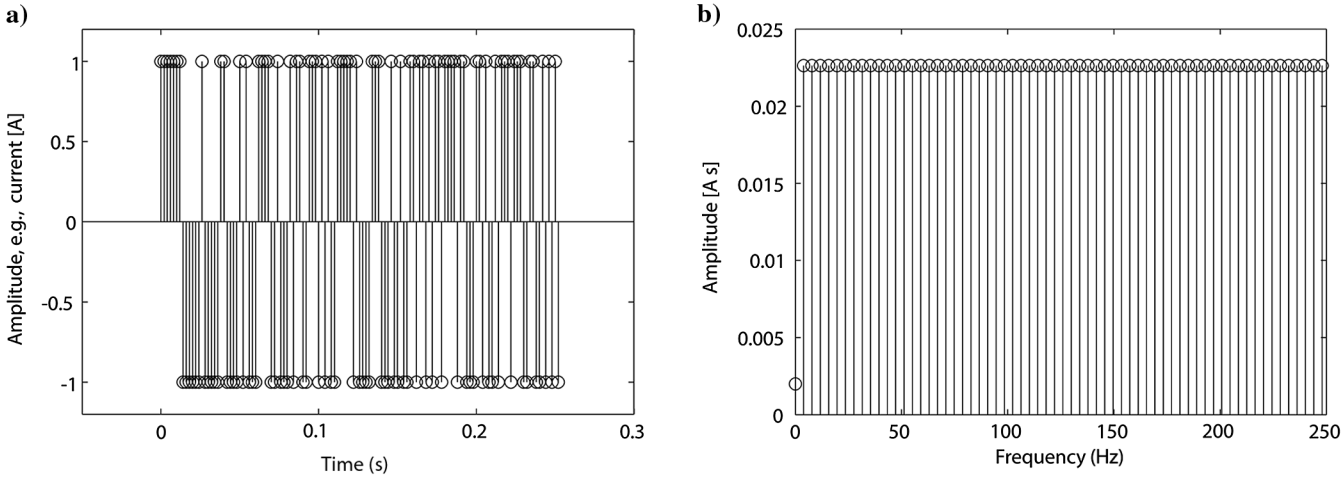

Figure 4. (a) Individual samples of order 7 PRBS, with amplitude in current [A], 2 ms sample interval; (b) its amplitude spectrum.

Convolution and deconvolution with PRBS signature and air gun signature

Figure 6a shows the result of convolving the traces of the wedge model with the PRBS signature of Figure 4a and the result appears to be very confused; it is very difficult to see the two events. Figure 6b shows the result of convolving the traces of the wedge model with the air gun signature. The two events can clearly be seen, followed by the subsequent bubble oscillations.

The proposed Wiener filter is designed to recover the impulse response of the earth, or Green's function. Application to the synthetic data of Figure 6a using the PRBS signature of Figure 4a as input gives the excellent result of Figure 7a. The quality factor for all traces is 1; that is, it is perfect. This is to be expected because the PRBS has no zeros in its amplitude spectrum and no white noise stabilization is necessary. Application to the synthetic data of Figure 6b using the air gun signature of Figure 5a as input is shown in Figure 7b. It is an excellent result, with the airgun bubble oscillations suppressed and with a quality factor in the range 0.9990–0.9994 on all traces, but it is not as good as the PRBS result because a small amount (0.1%) of white noise stabilization was required to stabilize the results at frequencies above 240 Hz, where the signature amplitudes are very small.

Figure 8a shows the estimated noise on Trace 1 of Figure 7b. This is the uncorrelated part of the trace and is introduced by the white noise stabilization. Its spectrum is shown in Figure 8b and is close to a scaled version of $1/|SA_k|$, where $|SA_k|$ is shown in Figure 5b. The stabilization is required because the amplitude spectrum of the signature is close to zero at certain frequencies, especially at the Nyquist frequency and just below.

In summary, perfect retrieval of the Green's function is possible if (1) there is no noise, (2) the source signature is known exactly,

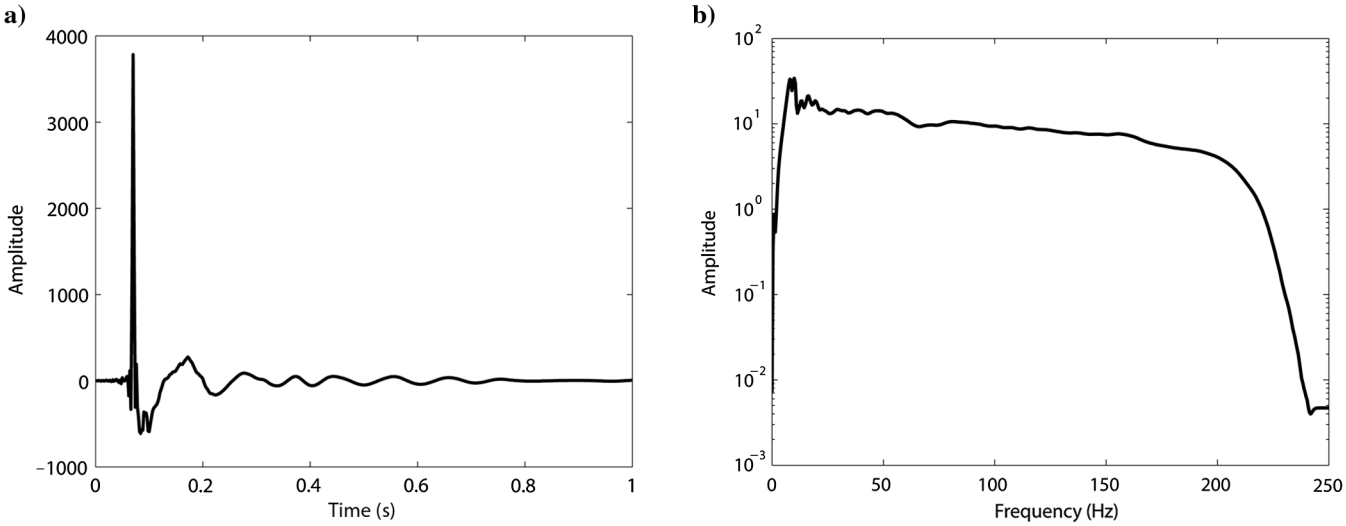

Figure 5. (a) Air gun signature, 2-ms samples; (b) its amplitude spectrum.

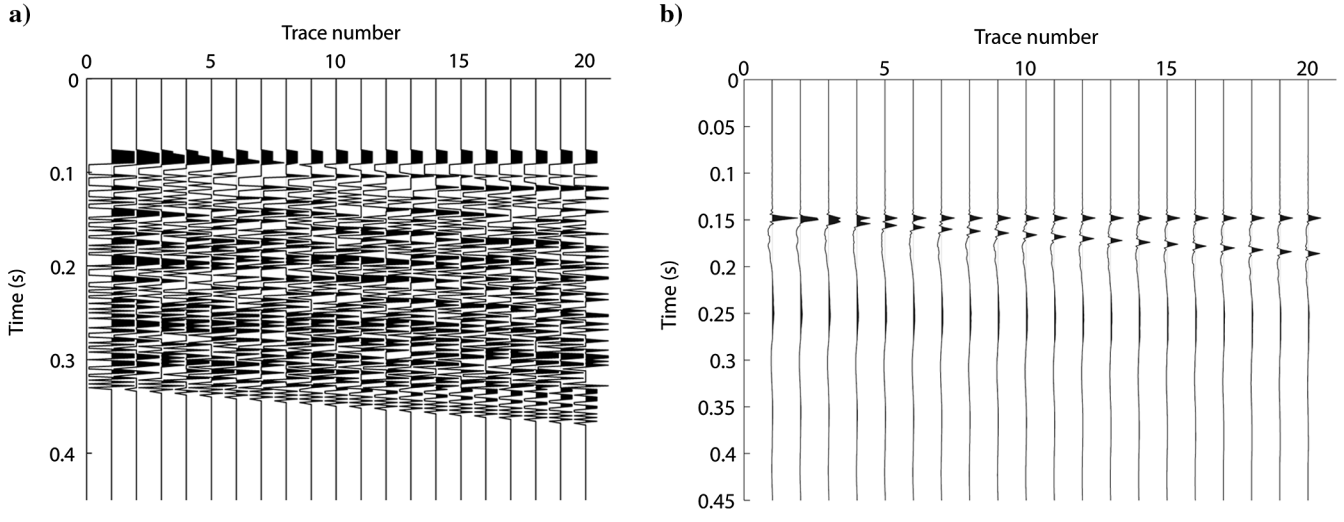

Figure 6. (a) Trace-by-trace convolution of PRBS with wedge model; (b) trace-by-trace convolution of air gun signature with wedge model.

(3) the amplitude spectrum of the source signature has energy in all frequencies, and (4) the response V_t is a complete convolution. In the examples presented above, this last condition is satisfied. In real data, it is normally not satisfied, especially in the seismic case, because the impulse response is always longer than the recorded data due to infinitely long trains of multiples, or reverberations.

EFFECT OF NOISE

Figure 9 shows the effect of noise on synthetic data using the PRBS source signature. Figure 9a shows the result of convolution of the wedge model with the PRBS signature, after which uncorrelated noise is added. The noise is generated independently for each trace as a sequence of normally distributed pseudorandom numbers. The added noise is shown separately in Figure 9f. The deconvolution result is shown in Figure 9b; white noise stabilization was not required. This result compares well with the original model, shown on the same amplitude scale in Figure 9d. The correlated part of the signal is shown in Figure 9c and the uncorrelated part, or estimated noise, is shown in Figure 9e. The estimated noise and the added noise are similar and do not appear to be correlated with the source signature or the model. There are differences, however, and these differences arise as follows. The added noise is in the desired output V_t, according to equation 1, and is therefore in the right-hand side crosscorrelation coefficients B_τ of the normal equations 17 for every trace. This causes errors in every sample of the estimated Green's function $\hat{g}_t$, on every trace, as shown in Figure 9b, even though the source signature is known perfectly in this example. Convolution of the estimated Green's function with the source signature yields the result shown in 9c. Comparing 9c and 9a, there is a clear reduction

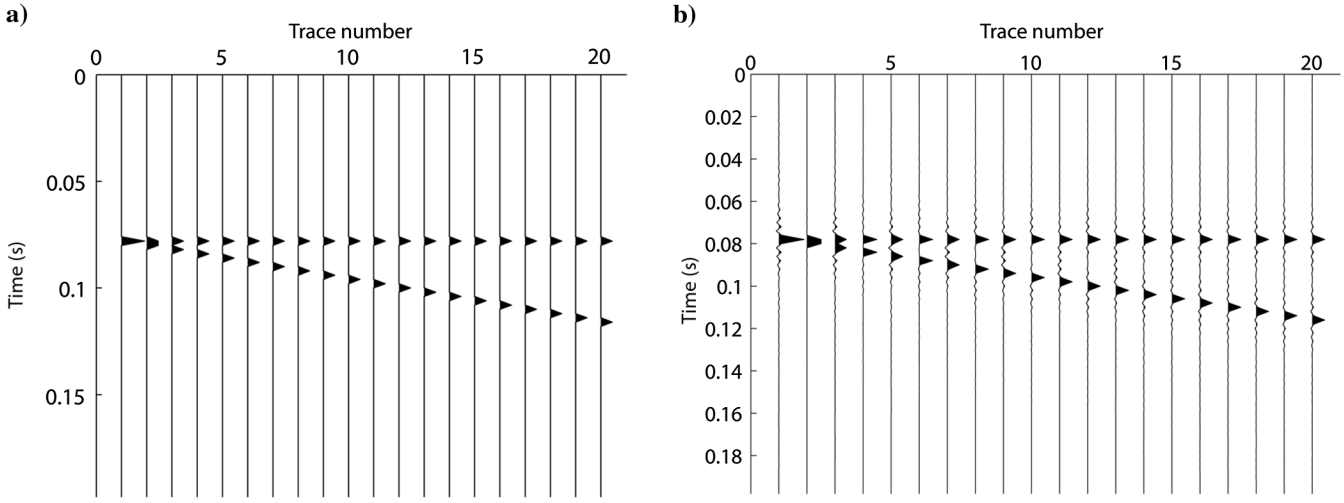

Figure 7. (a) Deconvolution of data in Figure 6a with PRBS signature of Figure 4a, no white noise stabilization; (b) deconvolution of data in Figure 6b with airgun signature of Figure 5a, with 0.1% white noise stabilization.

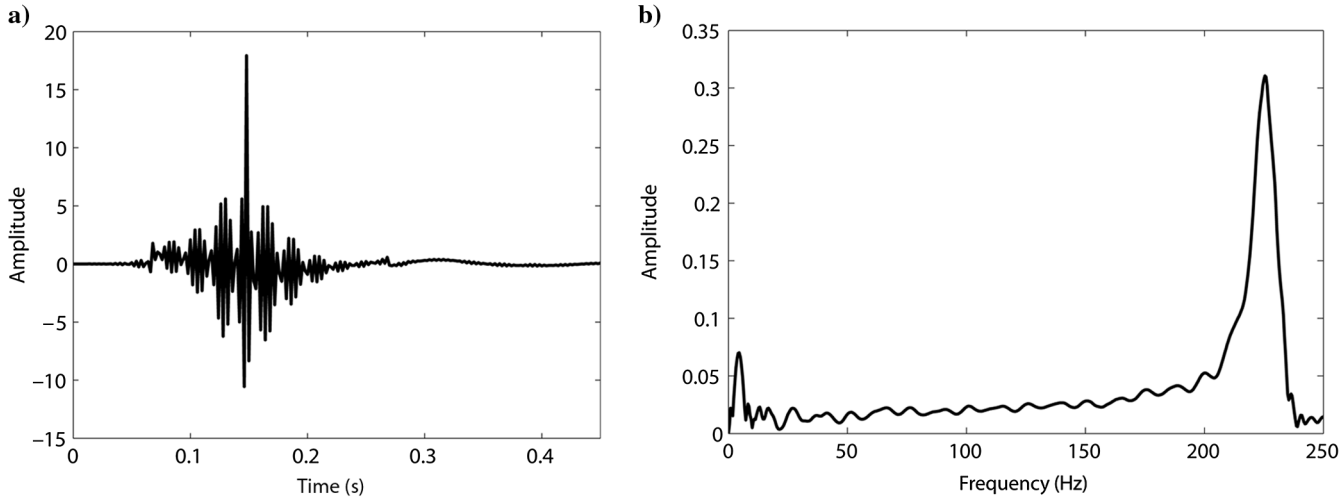

Figure 8. (a) Estimated noise on Trace 1 of Figure 6b: This is the uncorrelated part and is introduced by the white noise stabilization; (b) amplitude spectrum of (a).

in the noise level. The trace-by-trace difference in 9a–9c is shown in 9e and is not identical with the added noise component of 9a, shown in 9f.

The Wiener filtering operation does a good job at separating the signal and noise. The quality factors for the filters ranged from 0.956 on trace 20 to 0.976 on trace 1.

What is a good quality factor? If the signature is known perfectly, as in this case, the quality factor is limited only by the added noise, n_t in equation 1. Applying equation 15 to the normal equations 17 yields

$$q = \sum_{\tau=0}^{n} \hat{g}_\tau B_\tau.$$

There is a clear gain in signal-to-noise ratio (S/N). The compression of a PRBS of N samples to an impulse of 1 sample concentrates

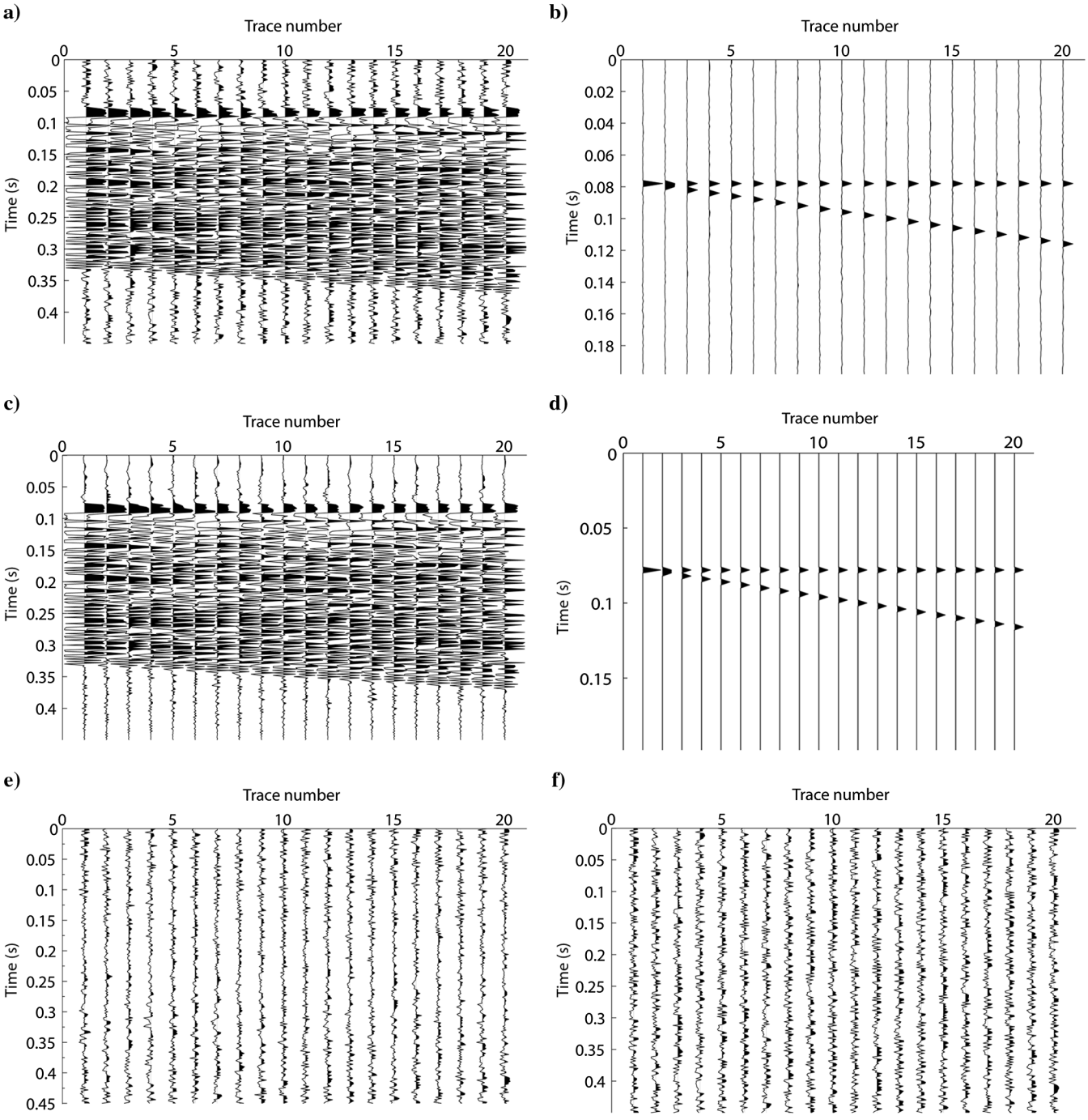

Figure 9. (a) Convolution of wedge model with PRBS, plus noise; (b) deconvolution of (a) with PRBS signature shown in Figure 4a; (c) correlated part of (a): the result of convolving PRBS of Figure 4a with result (b); (d) true wedge model on same plot scale as (b); (e) estimated noise: result of subtracting (c) from (a); (f) noise added in (a).

the energy of the N-length signal into a single sample, giving a gain in signal amplitude of $\sqrt{N}$. Because the amplitude spectrum of the impulse and the PRBS are almost identical, except at DC, the effect is confined to the phase spectrum. If the noise is white and random with zero mean, and uncorrelated with the PRBS, its amplitude would be unaffected by this process. We would therefore expect the S/N to increase by $\sqrt{N}$ in this case. For $N = 127$, this would be a gain of 11.27, or 21 dB. For noise with other characteristics, the gain in S/N would be different.

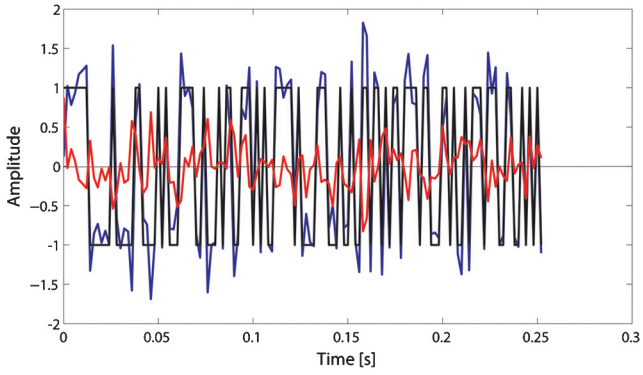

Figure 10. PRBS signature (black); error signal (red); PRBS minus error (blue).

EFFECT OF SIGNATURE ERRORS

Figure 10 shows the PRBS signature s_t in black, an error signal es_t in red, and the difference signal $\hat{s}_t = s_t - es_t$ in blue. The error signal consists of normally distributed pseudorandom numbers generated in a computer. Using $\hat{s}_t$ as the "estimated source signature" for deconvolution of the noise-free wedge model data gives the result shown in Figure 11b, in which no white noise stabilization was required and quality numbers in the range 0.956–0.970 were obtained. That is, approximately 96% of the energy is correlated with the estimated signature and approximately 4% is uncorrelated. Figure 11a shows the synthetic noise-free data, Figure 11c shows the part of the data that is correlated with the estimated source signature, and Figure 11d shows the difference between Figure 11a and 11c: the estimated noise.

Notice that the noise is strongly correlated from trace to trace. The effect of the errors in the estimated signature is to leave some of the data undeconvolved. The ratio of the deconvolved energy to undeconvolved energy is about 0.96/0.04 or 27 dB.

There are situations in which noise is correlated from trace to trace in common source gathers. In controlled-source electromagnetic data, for example, magnetotelluric noise is correlated across

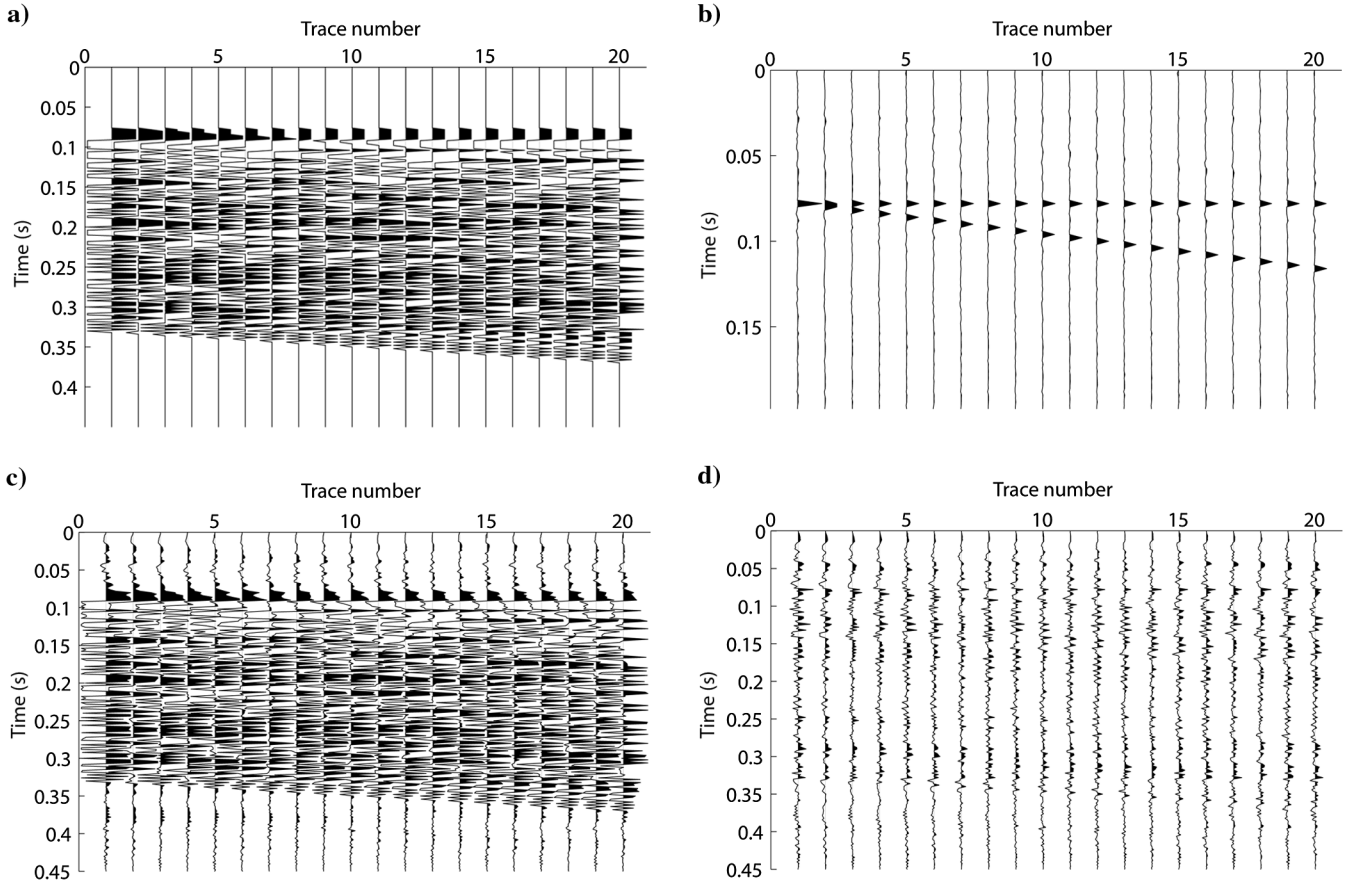

Figure 11. Result of deconvolution with errors in estimated signature. (a) Wedge model convolved with PRBS; (b) deconvolution of (a) using estimated signature of Figure 10; (c) correlated part of (a); (d) uncorrelated part of (a) — estimated noise.

traces acquired simultaneously and this knowledge can be used to attenuate the noise (Ziolkowski et al., 2010). To distinguish this kind of noise from noise that is caused by errors in the source signature estimate, it would be better to use common midpoint gathers, in which every trace is obtained at a different time from a different source and different receiver.

APPLICATION TO MARINE SEISMIC DATA

Figure 12a shows part of a shot record from a marine seismic survey in which the receiver ghost has been removed; that is, the data show the upward-traveling pressure wave at the receiver. The wave reflected from the sea surface has been removed. Figure 12b shows a magnification of part of Figure 12a. For Wiener estimation of the impulse responses in these data, the estimated source signature shown in Figure 5a was used, after removing the first 28 samples. Figure 12c shows the result, which was obtained with 0.1% added white noise. The operation improves the resolution of the data, as expected. This may be seen more clearly in the magnification, Figure 12d. As already demonstrated above on synthetic data, this source signature has excellent resolution. The purpose of the present test is to determine how well this estimated signature represents the true signature.

Figure 13 shows the variation in quality factor for this shot record. The quality is excellent: greater than 0.996 for all traces, and greater than 0.9995 for most of traces. (The quality factor drops to 0.996 on Trace 9, which represents a very small additional amount

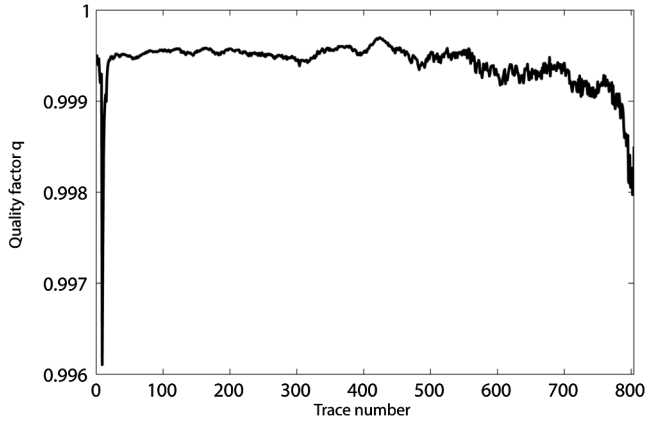

Figure 13. Quality factor as a function of trace number.

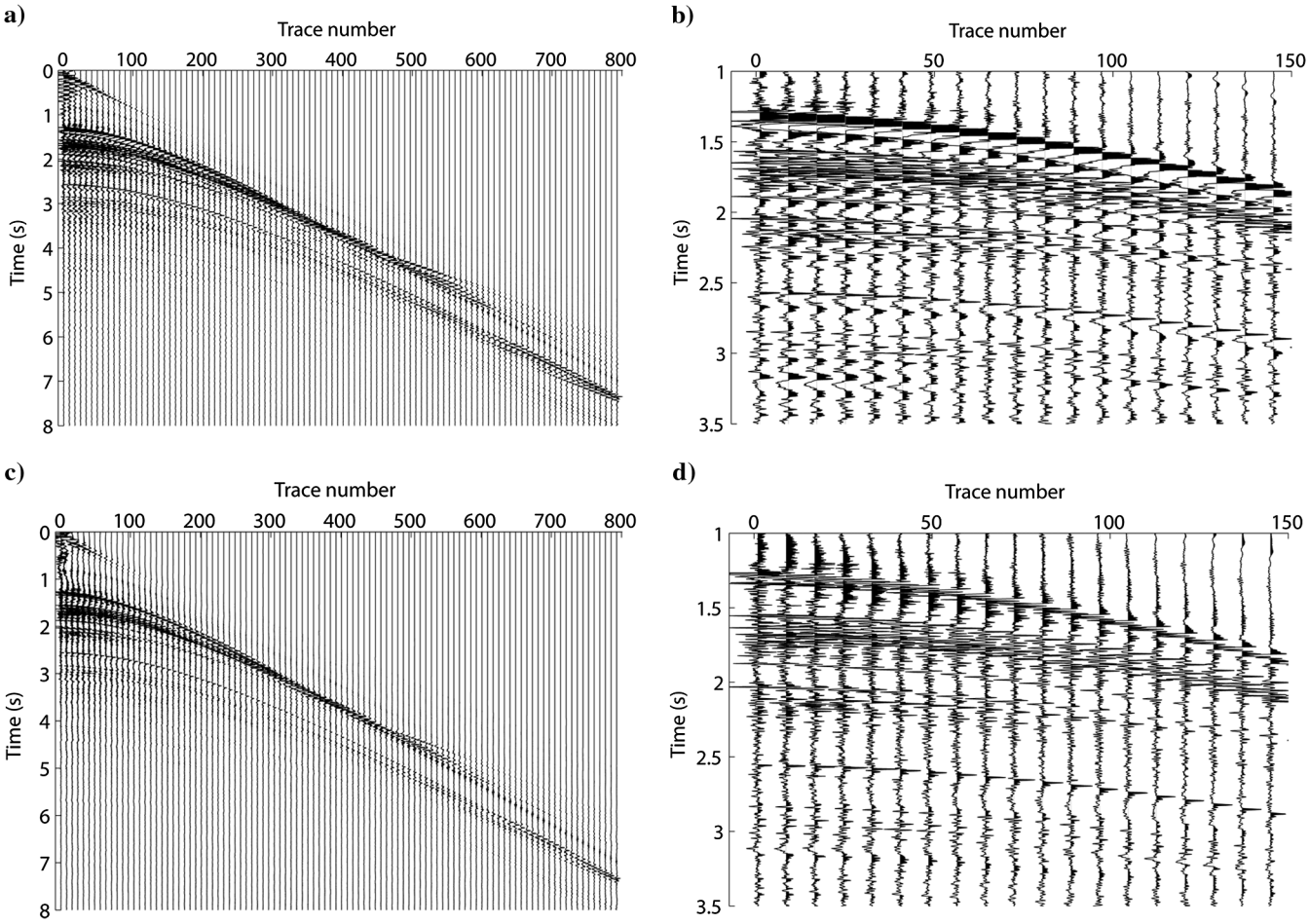

Figure 12. (a) Part of shot record, showing every eighth trace of raw data; (b) a smaller piece of (a); (c) the result of Wiener signature deconvolution of (a); (d) a smaller piece of (c) corresponding to (b).

of noise. It is too small to see on the raw data.) These numbers indicate that the source signature is a very accurate estimate of the true signature, because less than 0.4% of the energy on all traces is unaccounted for by the correlated part of the data, and on most traces this number is below 0.05%. The general form of Figure 13 is as expected. The source signature is estimated for the vertical direction. Because the inline dimensions of the source array (about 20 m) are not small compared with a wavelength at the higher

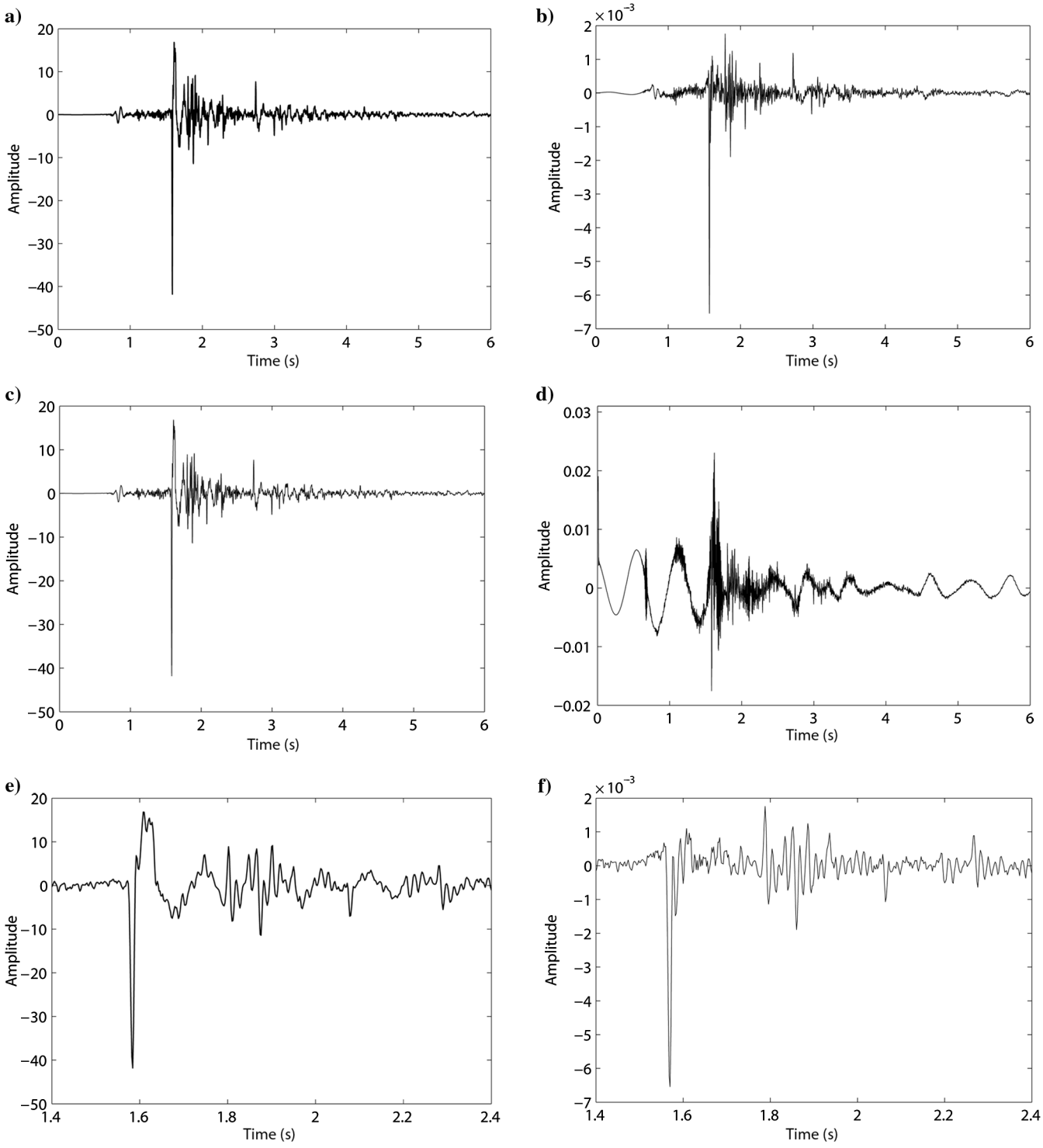

Figure 14. (a) Raw data: trace 100, Shot 1, 0–6 s; (b) estimated impulse response; (c) component correlated with the estimated source signature of Figure 5b; (d) component of (a) not correlated with the estimated source signature; (e) magnification of part of (a); (f) magnification of corresponding part of (b)

frequencies, the source is directional in the inline vertical plane, and the estimated vertical signature becomes increasingly in error as the angle of incidence increases. We therefore expect the quality factor to decrease gradually as the offset, and hence the angle of incidence, increases. This is exactly what we see in Figure 13, particularly for the highest offsets.

Figure 14 shows the result of impulse response estimation on a typical trace, Trace 100, of the shot record. Figure 14a shows the raw trace; Figure 14b shows the estimated earth impulse response, which has higher resolution than the original trace; Figure 14c is the component of (a) that is correlated with the estimated source signature, and Figure 14d is the difference between the raw trace and the correlated part. This part is uncorrelated with the estimated source signature and is therefore an estimate of the noise. Because the quality factor on Trace 100 is 0.9995, the ratio of correlated to uncorrelated energy is 9995:5 or 33 dB. Figure 14e shows a magnification of part of 14a, and Figure 14f shows a magnification of the corresponding part of 14b. Comparison of Figure 14e and 14f shows significant differences as the smoothing effect of the airgun signature is removed.

Figure 15 shows a display of the component of the shot gather uncorrelated with the estimated signature. This is the estimated noise. It looks like seismic data and is clearly correlated with the seismic response. As demonstrated with synthetic data above, it is caused by errors in the estimate of the source signature. These errors are very small, as shown above: about 30 dB less than the estimated signature. What is apparent in Figure 15, however, is that most of the uncorrelated component is in fact correlated with the seismic response. Any uncorrelated noise must be very small compared with this correlated noise. The quality of the signature deconvolution for these data is not limited by the noise in the data: it is limited by errors in the estimate of the source signature.

APPLICATION TO MARINE CSEM DATA

We now briefly consider the application of the method to fully towed marine transient controlled source electromagnetic data in which the source is an electric current dipole, the signature is one period of a PRBS, and the single receiver is an inline voltage dipole (Ziolkowski et al., 2011). Figure 16 shows a sequence of four records of (a) the measured source current and (b) the response at one receiver. The time between successive cycles is 120 s. Figure 17 shows the result of impulse response estimation for one trace. Figure 17 shows (a) the measured source current; (b) the measured electric field at the receiver; (c) the estimated earth impulse response; (d) the components of the measured response that are (blue) correlated with the source signature, and (red) uncorrelated with the source signature. No white noise stabilization was required. The quality factor for this example is 0.946.

The estimated noise in Figure 17d is rather low frequency. One candidate for this is magnetotelluric noise which increases dramatically at low frequencies (e.g., Ziolkowski and Wright, 2012). Another possibility, because this is a towed system, is noise generated at the receiver electrodes. A study of the electromagnetic noise is beyond the scope of this paper.

The estimated noise for the 48 traces in the line is displayed in Figure 18. There is no obvious correlation of the noise from trace to trace, indicating that the source signature estimate is excellent, as one would expect from the direct measurement of the source current. The limitation to the recovery of the earth impulse response is the noise. Errors in the source signature estimate, if any, are negligible in comparison.

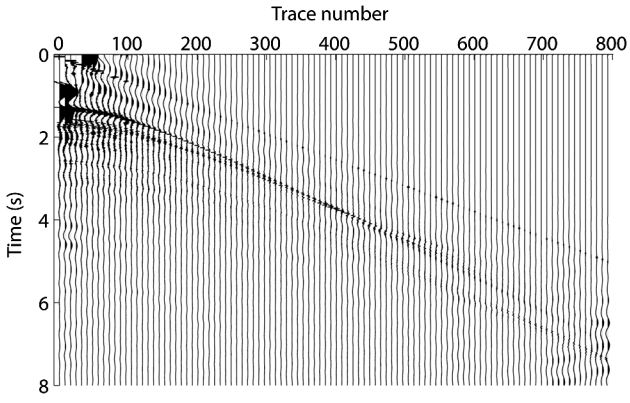

Figure 15. Part of shot record, showing every eighth trace of the component of the data uncorrelated with the estimated source signature.

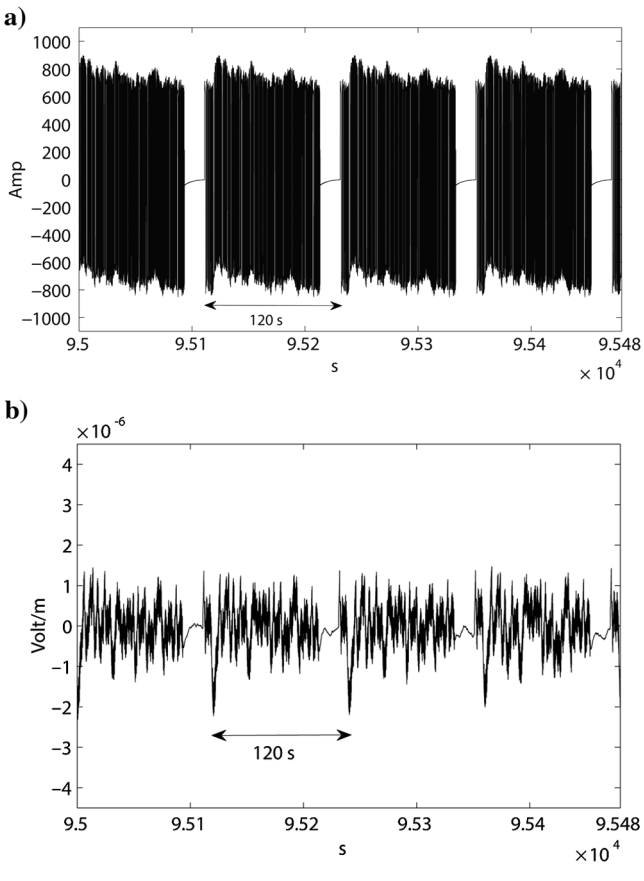

Figure 16. A portion of the towed streamer transient controlled source electromagnetic data: (a) measured source current (amps); (b) measured receiver response 2145 m behind source (V/m). The repetition time is 120 s.

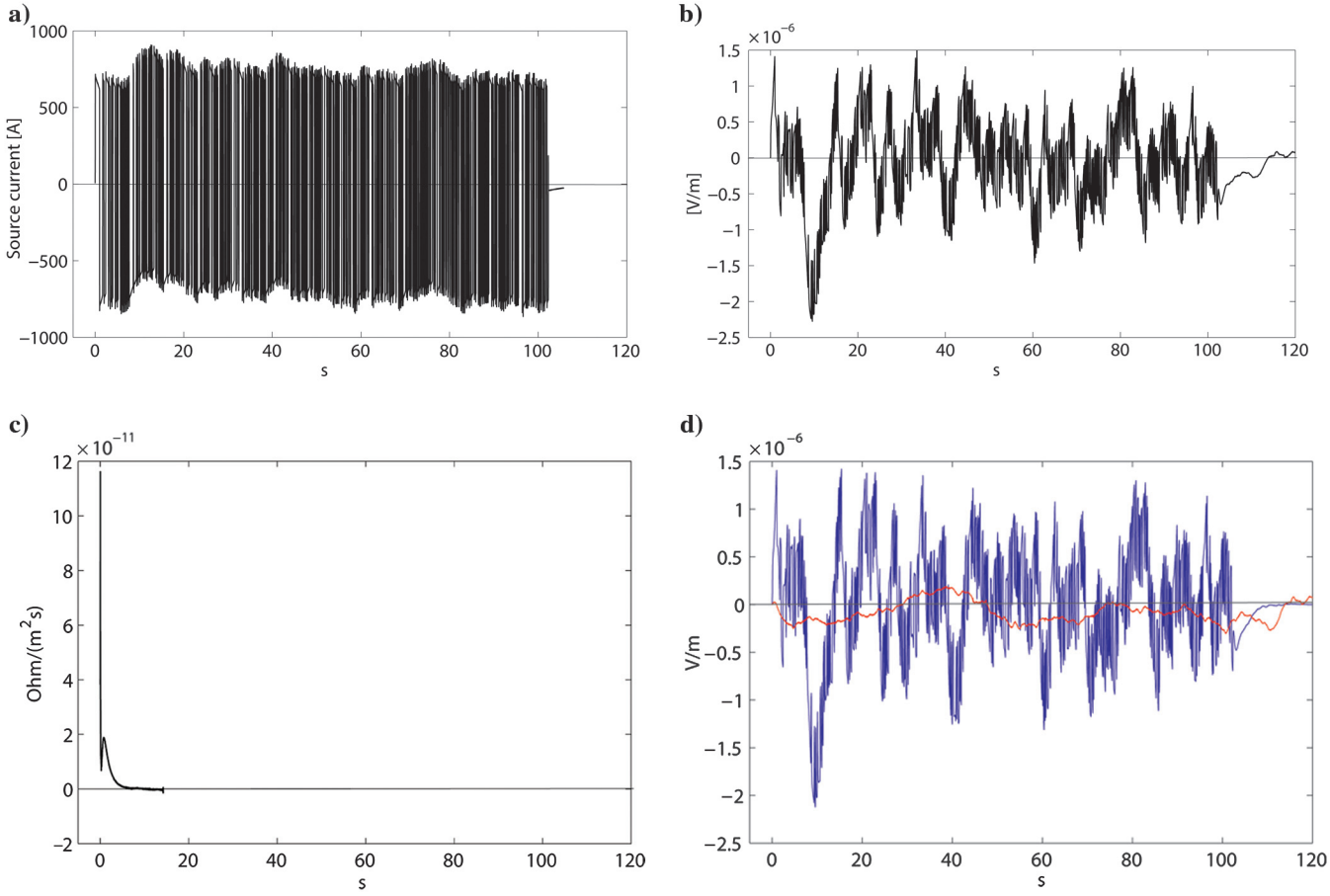

Figure 17. Deconvolution of one trace. (a) Measured source current (amps); (b) measured electric field at receiver (V/m); (c) estimated earth impulse response; (c) correlated and uncorrelated components of (b): blue curve is the correlated component, the convolution of (a) and (c); red curve is response (b) minus the correlated component.

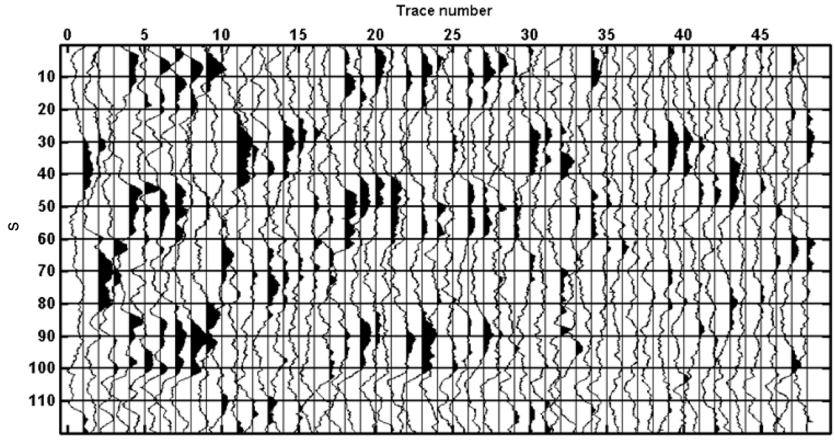

Figure 18. Display of the estimated noise on the receiver channel for the 48 successive records.

CONCLUSIONS

Classical signature deconvolution yields the earth impulse response, or Green's function, plus noise, provided the source signature is known precisely. Systematic errors in the estimate of the source signature lead to an additional noise term that is indistinguishable from signal and is unquantifiable.

By reformulating deconvolution as the problem of finding the optimum estimated earth impulse response, given the estimated source signature and measured output signal, we have separated out the portion of the signal that is correlated with the estimated source signature and have also obtained an estimate of the noise, which may contain remains of undeconvolved data. If this is the case, the errors in the signature estimate show up in

the estimated noise as signal that is correlated with the earth impulse response.

We have demonstrated the method on marine seismic data, and on marine transient electromagnetic data. For the marine seismic data example, the errors in source signature estimation were the limiting factor in recovery of the earth impulse response. For the marine transient electromagnetic data, the ambient noise was the limiting factor.

The method can be used to evaluate the quality of source signature estimates in signature deconvolution, as demonstrated here, and may be applied to other types of data including land vibroseis data and classical earthquake seismic data.

ACKNOWLEDGMENTS

I am very grateful to PGS and the Royal Academy of Engineering for supporting the research. I also thank PGS for permission to show the high-quality marine seismic and CSEM data. I thank Gregg Parkes for his suggestion that synthetics be included, and for pointing out the effect of source directivity on the quality of the signature deconvolution; I thank David Wright for his help in analyzing correlated noise; and I thank Guido Baeten and Peter Vermeer for helpful comments and suggestions on an oral version of the paper. Finally, I thank Associate Editor Jose Carcione, Reviewers Ian Moore and Huub Douma, and a third anonymous reviewer for their encouragement and very thoughtful comments and suggestions.

REFERENCES

Duncan, P. M., A. Hwang, R. N. Edwards, R. C. Bailey, and G. D. Garland, 1980, The development and applications of a wide band electromagnetic sounding system using a pseudo-noise source: Geophysics, **45**, 1276–1296, doi: 10.1190/1.1441124.

Fokkema, J. T., and A. M. Ziolkowski, 1987, The critical reflection theorem: Geophysics, **52**, 965–972, doi: 10.1190/1.1442365.

Golomb, S. W., 1955, Sequences with randomness properties: The Glenn L. Martin Company.

Golomb, S. W., 1982, Shift register sequences: Aegean Park Press.

Jovanovich, D. B., R. D. Sumner, and S. L. Akins-Easterlin, 1983, Ghosting and marine signature deconvolution: A prerequisite for detailed seismic interpretation: Geophysics, **48**, 1468–1485, doi: 10.1190/1.1441431.

Levinson, N., 1946, The Wiener RMS (root mean square) error criterion in filter design and prediction: Journal of Mathematical Physics, **25**, 261–278.

Osman, O. M., and E. A. Robinson, eds., 1996, Seismic source signature estimation and measurement: SEG.

Peacock, K. L., and S. Treitel, 1969, Predictive deconvolution: Theory and practice: Geophysics, **34**, 155–169, doi: 10.1190/1.1440003.

Rice, R. B., 1962, Inverse convolution filters: Geophysics, **27**, 4–18, doi: 10.1190/1.1438979.

Robinson, E. A., 1954, Predictive decomposition of time series with applications to seismic exploration: Ph.D. thesis, MIT.

Robinson, E. A., 1967, Statistical communication and detection with special reference to digital data processing of radar and seismic signals: Charles Griffin.

Robinson, E. A., and S. Treitel, 1967, Principles of digital Wiener filtering: Geophysical Prospecting, **15**, 311–332, doi: 10.1111/j.1365-2478.1967.tb01793.x.

Stoffa, P. L., and A. M. Ziolkowski, 1983, Seismic source decomposition: Geophysics, **48**, 1–11, doi: 10.1190/1.1441402.

Wiener, N., 1949, Extrapolation, interpolation and smoothing of stationary time series: John Wiley and Sons.

Zierler, N., 1959, Linear recurring sequences: Journal of the Society for Industrial and Applied Mathmatics, **7**, 31–48, doi: 10.1137/0107003.

Ziolkowski, A., 1984, Deconvolution: International Human Resources Development Corporation.

Ziolkowski, A., R. Parr, D. Wright, V. Nockles, C. Limond, E. Morris, and J. Linfoot, 2010, Multi-transient electromagnetic repeatability experiment over the North Sea Harding Field: Geophysical Prospecting, **58**, 1159–1176.

Ziolkowski, A., and D. Wright, 2012, The potential of the controlled source electromagnetic method: IEEE Signal Processing Magazine, 36–52, doi: 10.1109/MSP.2012.2192529.

Ziolkowski, A., D. Wright, and J. Mattsson, 2011, Comparison of pseudo-random binary sequence and square-wave transient controlled-source electromagnetic data over the Peon gas discovery, Norway: Geophysical Prospecting, **59**, 1114–1131, doi: 10.1111/j.1365-2478.2011.01006.x.